Journal of Hydrology 553 (2017) 549–558

Contents lists available at ScienceDirect

Journal of Hydrology

journal homepage: www.elsevier.com/locate/jhydrol

Research papers

# Modelling sheet erosion on steep slopes in the loess region of China

Bing Wu [a,c], Zhanli Wang [a,b,*], Qingwei Zhang [b], Nan Shen [b], June Liu [d]

[a] State Key Laboratory of Soil Erosion and Dryland Farming on the Loess Plateau, Institute of Soil and Water Conservation, Chinese Academy of Sciences and Ministry of Water Resources, Yangling, Shaanxi 712100, China
[b] State Key Laboratory of Soil Erosion and Dryland Farming on the Loess Plateau, Institute of Soil and Water Conservation, Northwest A&F University, Yangling, Shaanxi 712100, China
[c] University of Chinese Academy of Sciences, Beijing 100049, China
[d] School of Geography and Tourism, Shaanxi Normal University, Xi'an, Shaanxi 710119, China

ARTICLE INFO

*Article history:*
Received 14 November 2016
Received in revised form 24 June 2017
Accepted 10 July 2017
Available online 19 July 2017
This manuscript was handled by P. Kitanidis, Editor-in-Chief, with the assistance of Ioannis K. Tsanis, Associate Editor

*Keywords:*
Sheet erosion rate
Rainfall intensity
Slope gradient
Flow velocity
Hydrodynamic parameters

ABSTRACT

The relationship of sheet erosion rate (*SE*), slope gradient (*S*) and rainfall intensity (*I*), and hydraulic parameters, such as flow velocity (*V*), shear stress ($\tau$), stream power ($\Omega$) and unit stream power (*P*), was investigated to derive an accurate experimental model. The experiment was conducted at slopes of 12.23%, 17.63%, 26.8%, 36.4%, 40.4% and 46.63% under I of 48, 60, 90, 120, 138 and 150 mm $h^{-1}$, respectively, using simulated rainfall. Results showed that sheet erosion rate increased as a power function with rainfall intensity and slope gradient with $R^2 = 0.95$ and Nash–Sutcliffe model efficiency (*NSE*) = 0.87. Sheet erosion rate was more sensitive to rainfall intensity than to slope gradient. It increased as a power function with flow velocity, which was satisfactory for predicting sheet erosion rate with $R^2 = 0.95$ and *NSE* = 0.81. Shear stress and stream power could be used to predict sheet erosion rate accurately with a linear function equation. Stream power ($R^2 = 0.97$, *NSE* = 0.97) was a better predictor of sheet erosion rather than shear stress ($R^2 = 0.90$, *NSE* = 0.89). However, a prediction based on unit stream power was poor. The new equation (i.e. $SE = 7.5 \times 10^{12} S^{1.43} I^{3.04}$ and $SE = 0.06\Omega - 0.0003$ and $SE = 0.011\tau - 0.01$) would improve water erosion estimation on loess hillslopes of China.



## 1. Introduction

The Loess Plateau in China is one of the regions in the world that is experiencing serious soil erosion (Shi and Shao, 2000; Zhang et al., 2009; Liu et al., 2012b; Zhao et al., 2013). Sheet erosion is one of the major erosion processes in the Loess Plateau (Liu et al., 2012a); thus, a sheet erosion model must be established to aid in the decision-making process regarding soil erosion control in this area.

A number of process-based soil erosion prediction models are credible for assessing erosion rate in a particular area. These models include the Water Erosion Prediction Project (Nearing et al., 1989), the Griffith University Erosion System Template (Misra and Rose, 1996), the European Soil Erosion Model (Morgan et al., 1998) and the ANSWERS model (Beasley and Huggins, 1982). In addition, rainfall intensity (*I*) or flow discharge and slope gradient (*S*) have been used to predict sheet erosion rate (*SE*), and the relationship between sheet erosion rate, rainfall intensity (or flow discharge) and slope gradient has been evaluated (Beasley and Huggins, 1982; McCool et al., 1987; Nearing et al., 1989; Kinnell, 1993; Liu et al., 1994; Zhang and Hosoyamada, 1996; Zhang et al., 1998; Bulygin et al., 2002).Nearing et al. (1989) discovered that a power function exist between sheet erosion rate and rainfall intensity, and that sheet erosion rate varied directly with the square of rainfall intensity ($I^2$). Kinnell (1993) observed that sheet erosion rate varied directly with rainfall intensity

*Abbreviations:* ***SE***, the mean sheet erosion rate (kg $m^{-2}$ $s^{-1}$); $\boldsymbol{t_i}$, , the sampling time (s); $\boldsymbol{m_i}$, the weight of sediments during sampling time (kg); ***L***, the length and the width of the test plot (m); ***W***, the length and the width of the test plot (m); ***S***, the slope gradient (%); ***I***, the rainfall intensity (mm $h^{-1}$); ***V***, the mean flow velocity (m $s^{-1}$); $\boldsymbol{V_s}$, the surface flow velocity (m $s^{-1}$); ***k***, the correction coefficient; **h**, the mean flow depth (m); $\boldsymbol{R_i}$, the weight of the runoff during sampling time (kg); $\boldsymbol{\rho_i}$, the mass density of the runoff (kg $m^{-3}$); $\boldsymbol{\rho s}$, the mass density of the sediments (=2650 kg $m^{-3}$); ***P***, the water mass density (kg $m^{-3}$); ***g***, the gravitational constant (m $s^{-2}$); $\boldsymbol{S_i}$, the sine of the bed slope (m $m^{-1}$); $\boldsymbol{\tau}$, the flow shear stress (Pa); $\boldsymbol{\Omega}$, the stream power (W $m^{-2}$); ***P***, the unit stream power (m $s^{-1}$); ***N***, the Manning roughness; ***R***, the hydraulic radius (m); ***NSE***, the Nash-Sutcliffe efficiency; ***RE***, the relative error; ***RME***, the average absolute values of the relative error (%); $\boldsymbol{R^2}$, the coefficient of determination; $\boldsymbol{O_i}$, the observed values (kg $m^{-2}$ $s^{-1}$); $\boldsymbol{P_i}$, the predicted values (kg $m^{-2}$ $s^{-1}$); $\overline{\boldsymbol{O}}$, the mean of the observed value (kg $m^{-2}$ $s^{-1}$); $\overline{\boldsymbol{P}}$, the mean of the predicted value (kg $m^{-2}$ $s^{-1}$); ***n***, the number of samples.

* Corresponding author at: State Key Laboratory of Soil Erosion and Dryland Farming on the Loess Plateau, Institute of Soil and Water Conservation, Chinese Academy of Sciences and Ministry of Water Resources, Yangling, Shaanxi 712100, China.

*E-mail address:* zwang@nwsuaf.edu.cn (Z. Wang).

http://dx.doi.org/10.1016/j.jhydrol.2017.07.017
0022-1694/

rather than $I^2$ when factors, such as flow discharge, were also considered. This finding is consistent with the report of other researchers (Beasley and Huggins, 1982; Zhang et al., 1998; Bulygin et al., 2002). Zhang et al. (1998) suggested that sheet erosion rate had been predicted to be a power function of slope gradient percentage. McCool et al. (1987) found that sheet erosion rate had been predicted to be a linear function of the sine of slope gradient. This finding is consistent with the report of Liu et al. (1994). Zhang and Hosoyamada (1996) suggested that sheet erosion rate had been predicted to be a polynomial function of slope gradient's sine.

In addition, Moss (1988) and Kinnell (1990) suggested that sheet erosion rate would be expected to vary directly with flow velocity for a given soil type and rainfall intensity. Cantalice et al. (2016) conducted an experiment on slopes of 15%, 25%, 35% and 45%; they observed that flow velocity in a pasture varied significantly with the increase in slope and increased erosion rates until the 35% slope. Al-Durrah and Bradford (1981) found that shear stress was a valuable parameter in the prediction model in studies regarding interrill erodibility factors. Furthermore, many researchers have investigated new models to estimate sheet erosion rate with hydraulic parameters and to analyse the influence of different hydraulic parameters, such as mean flow velocity ($V$) (Fox and Bryan, 2000), shear stress ($\tau$) (Fan and Wu, 1999), stream power ($\Omega$) (Huang, 1995; Cao et al., 2015) and unit stream power ($P$) (Fox and Bryan, 2000), on sheet erosion rate. (Table 1).

The Loess Plateau in northwest China is characterised by steep slopes and experiences high rain intensities. Govers (1992) determined that no existing formula could perform efficiently over the entire range of available data. Hence, experimental data for this region are necessary.

The objectives of this study are as follows:

(1) to understand the effects of slope gradient, rainfall intensity and flow velocity on sheet erosion rate;
(2) to evaluate the relationships between sheet erosion rate and hydrodynamic parameters; and
(3) to establish new and more accurate experimental models of sheet erosion rate for loess regions.

## 2. Materials and methods

### 2.1. Experiment equipment

#### 2.1.1. Simulated rainfall device

The experiments were conducted in the Simulation Rainfall Hall operated by the State Key Laboratory of Soil Erosion and Dryland Farming on the Loess Plateau at the Institute of Soil and Water Conservation, Chinese Academy of Sciences and the Ministry of Water Resources in Yangling, Shaanxi Province, China. A rainfall simulator system with nozzles on two sides was used to reproduce simulated rainfall (Fig. 1). This rainfall simulator could be set to any selected rainfall intensity by changing water pressure and nozzle size. The rainfall intensities used for this study ranged from 48 mm $h^{-1}$ to 150 mm $h^{-1}$. The fall height of raindrops sprayed from the nozzles was approximately 16 m above the soil surface in all the experiments. The raindrop diameter of the simulated rainfall were from 0.125 mm to 6.0 mm, moreover, the raindrop median volume diameters were from 1.52 mm to 2.7 mm. The dispersed raindrop of different diameters were precisely created by adjusting the aperture of the nozzle orifice and the water pressure. The simulated rainfall, with uniformity higher than 90%, exhibited similar raindrop size and distribution to natural rainfall, which was consistent with that reported by Shen et al. (2016).

#### 2.1.2. Experiment soil pan

Each experiment soil pan with metal frames was 140 cm long, 120 cm wide and 25 cm deep. The slope gradient for the soil pan could be adjusted between 0% and 84%. The test plot, which was the collection area of runoff and sheet erosion, was 80 cm long, 60 cm wide and 25 cm deep. A 35 cm-wide border area around the test plot was filled with soil in the same manner as the test plot to equalise the opportunity for splash onto and off the plots, which was consistent with the soil pan reported by Mayer et al. (1989) (Fig. 1).

### 2.2. The study area and test soil

The study area was located in Ansai County (109 °19′ E, 36 °51′ N), Shaanxi Province in China, is a typical loessial region with hills

**Table 1**
Models applied to predict sheet erosion rate with hydraulic parameters.

| Researchers | Used hydraulic parameter | Model | Model type | Slope gradient |
|---|---|---|---|---|
| Fox and Bryan (2000) | Flow velocity | SE = 2.17 V + 0.24 | Linear function | 2.5%–40% |
| Cao et al. (2015) | Stream power | SE = 0.00008Ω-0.00079 | Linear function | 10.5%–26.8% |
| Huang (1995) | Stream power | SE = 0.502Ω-0.838 | Linear function | 4%–20% |
| Fan and Wu (1999) | Shear stress | $SE = a\tau^{(-1.3\sim0.97)}$ | Power function | 10%–100% |
| Fox and Bryan (2000) | Unit stream power | SE = 4.45 P + 2.54 | Linear function | 2.5%–40% |

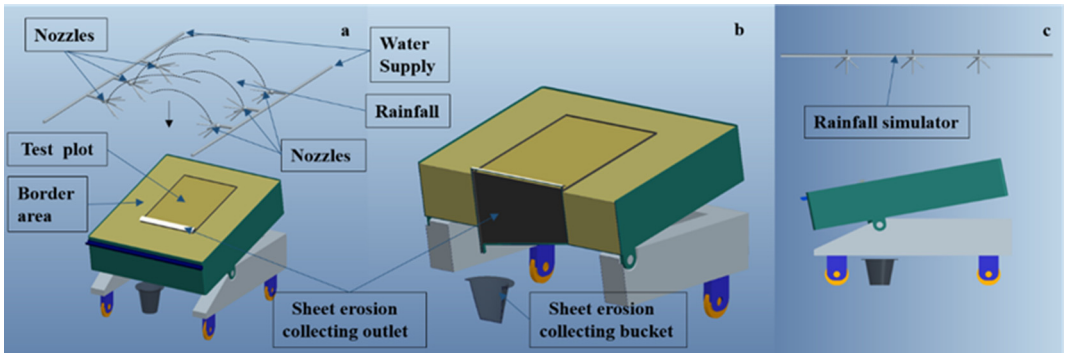


**Fig. 1.** The experimental setup and rainfall Simulator.

and gullies on the Loess Plateau. Mean altitude of the region is approximately 1200 m. The region has a typical semiarid continental climate, with an average annual temperature of 8.8 °C and mean annual precipitation of 500 mm approximately, 60% or more of which falls between July and September, typically in high-intensity rainstorms. The soil is classified as a typical loessial soil, representing the most common soil type on the Loess Plateau, being highly erodible and very susceptible to the erosive forces. More than 30% of land are cropland. The land cover have shown in Fig. 2.

The test soil was collected from a depth of 0 cm–25 cm at the farming layer of cropland. It consisted of 70.09% sand (diameter: 0.02–2.0 mm), 21.42% silt (diameter: 0.002–0.02 mm) and 8.49% clay (diameter: <0.002 mm), thus the test soil was sandy loam based on the soil texture classification system of United States Department of Agriculture (Huang and Zhan, 2002). The average diameter of the test soil was 0.039 mm. the particle size distribution of test soil was shown in Fig. 3.

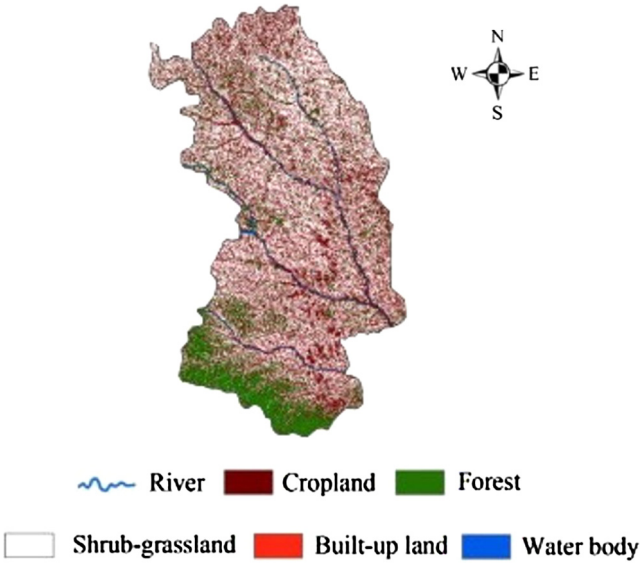


**Fig. 2.** The land cover of Ansai County, Shaanxi Province in China.

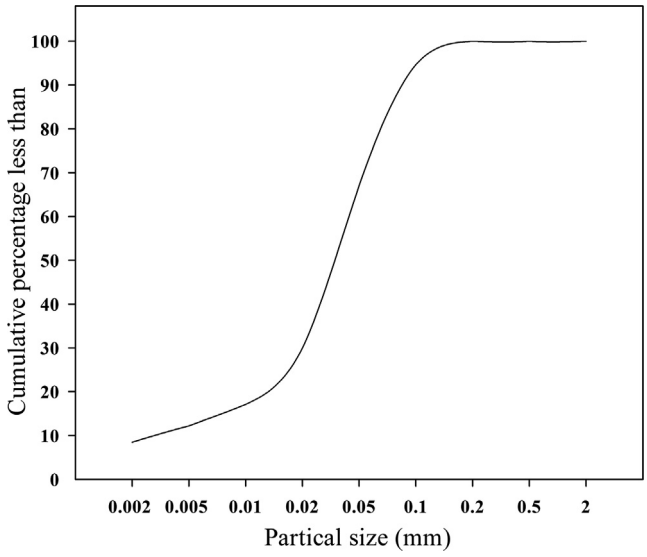


**Fig. 3.** The particle size distribution of test soil.

### 2.3. Experiment setup

The experimental treatments used in this study included complete combination of six rainfall intensities (48, 60, 90, 120, 138 and 150 mm $h^{-1}$) and six slope gradients (12.23%, 17.63%, 26.8%, 36.4%, 40.40% and 46.63%), i.e., 36 combinations of rainfall intensities and six slope gradients. For an experiment of each combination of rainfall intensity and slope gradient, 2 replicate were undertaken. Before packing the soil, its water content was adjusted to 14%, which was the typical level during the flood season on the Loess Plateau when most erosion would occur (Liu et al., 2014). A bulk density of 1.2 g $cm^{-3}$ (measured via a cutting ring in compacted state) was selected for the study. Firstly, a 5 cm-thick sand layer was packed at the bottom of the soil pan, which allowed free drainage of excess water. The $D_{50}$ of natural sand is 0.39 mm, with 2.58% clay (<0.002 mm), 3.94% silt (0.002–0.02 mm), fine sand 17.31% (0.02–0.2 mm) and coarse sand 76.17% (0.2–2 mm). The total porosity was 49% and the saturated hydraulic conductivity was 5.91 mm $min^{-1}$. Then, the test soil was packed in the soil pan over the sand layer. The soil was packed to a depth of 20 cm. In order to compact the test soil to the same degree, the test soil was packed in four 5 cm layers. Firstly, the soil amount of each layer was kept as constant as possible to maintain similar bulk density and uniform spatial distribution of soil particles. Secondly, the test soil of each packed soil layer was compacted to the designed bulk density before the next layer was packed to ensure uniformity in the soil structure. The metal outlets at the lower end allowed the collection of sheet erosion.

### 2.4. Experiment procedures

After preparing the soil pan, the experimental soil pan was pre-wetted with 25 mm $h^{-1}$ rainfall intensity, which lasted for approximately 30 min. This pre-rain phase with a nylon net cover over the soil pan was designed to create uniform soil surface moisture conditions and to reduce variability in soil surface micro relief developed during the packing process, which was consistent with the method reported by An et al. (2012). Then, one day (i.e. 24 h) after the pre-rain phase, the slope gradient and rainfall intensity of the soil pan were adjusted to the levels required for this study and the simulated rainfall experiment began to be done.

In the process of simulated rainfall experiment for each combination of slope gradient and rainfall intensity, samples of runoff produced by simulated rainfall were first collected for 1 min and 2 min after the onset of the runoff, and then for every 3 min until the end of the simulated rainfall experiment. For individual rainfall experiment under each combination of slope gradient and rainfall intensity, 15 runoff samples were collected, thus 15 measurement data were obtained. As 2 replicate were undertaken for individual rainfall experiment of each combination of rainfall intensity and slope gradient, so 30 measurement data were totally obtained for individual rainfall experiment of each combination of rainfall intensity and slope gradient with 2 replicate.

In addition to sampling runoff, flow velocity was measured using $KMnO_4$ as a tracer. The time during which the tracer was required to traverse a marked distance (50 cm) was determined based on the colour-front propagation using a stop watch. Surface flow velocity was measured 15 times for each treatment of individual rainfall event and 2 surface flow velocities values were obtained from the left and right of the test plot each time. The runoff samples were weighed and left to sit to allow suspended particles to settle. The clear supernatant was decanted and the sediments left were oven-dried at 105 °C for 24 h to determine sediment weight. Sheet erosion rate was defined as sediment weight per unit area per unit time.

### 2.5. Determination of date

#### 2.5.1. Sheet erosion rate

Using 30 measurement data obtained for individual rainfall experiment of each combination of rainfall intensity and slope gradient with 2 replicate, we calculated and obtained 1 data of the mean sheet erosion rate (*SE*) for individual rainfall experiment event under each combination of slope gradient and rainfall intensity. Thus, 36 data of the mean sheet erosion rates (*SE*) for 36 individual rainfall experiment events under 36 combinations of slope gradients and rainfall intensities were obtained. We used these 36 data of the mean sheet erosion rates (*SE*) for 36 individual rainfall experiment events to do all analysis.

For each combination of slope gradient and rainfall intensity, the formula that 30 sheet erosion rate values were used to calculate the mean sheet erosion rate (*SE*) of individual event is as follows:

$$SE = \frac{1}{30}\sum_{1}^{30}\frac{m_i}{LWt_i} \tag{1}$$

where *SE* is the mean sheet erosion rate (kg m$^{-2}$ s$^{-1}$), $t_i$ is the sampling time (s), $m_i$ is the weight of sediments during sampling time (kg), *L* and *W* are the length and the width of the test plot (m).

#### 2.5.2. Flow velocity

The value of surface flow velocity was used to estimate the mean flow velocity using the following formula:

$$V = kV_S \tag{2}$$

where *Vs* is the surface flow velocity (m s$^{-1}$); *V* is the mean flow velocity (m s$^{-1}$) and *k* is the correction coefficient, which is 0.67 for laminar flow, 0.7 for transitional flow and 0.8 for turbulent flow (Li and Abrahams 1999; An et al., 2012).

#### 2.5.3. Flow depth

For each combination of slope gradient and rainfall intensity, 30 flow depth values were used to calculate the mean flow depth (h) using the following formula:

$$h = \frac{1}{30}\sum_{1}^{30}\frac{R_i/\rho_i - m_i/\rho_s}{VWt_i} \tag{3}$$

where *h* is the mean flow depth (m), $R_i$ is the weight of the runoff during sampling time (i.e. $t_i$) (kg), $\rho_i$ is the mass density of the runoff (kg m$^{-3}$), $\rho_s$ is the mass density of the sediments (2650 kg m$^{-3}$), $m_i$ is the weight of the sediments during sampling time (kg), *V* is the mean flow velocity (m s$^{-1}$) and $t_i$ is the sampling time (s).

#### 2.5.4. Hydrodynamic parameters

Shear stress ($\tau$, measured in Pa; Nearing et al., 1991), stream power ($\Omega$, measured in W m$^{-2}$; Bagnold, 1966; Prosser and Rustomji, 2000) and unit stream power (*P*, measured in m s$^{-1}$; Yang, 1972, 1973) were calculated as

$$\tau = \rho g h S_i \tag{4}$$

where $\tau$ is the shear stress (Pa), $\rho$ is the water mass density (kg m$^{-3}$), *g* is the gravitational constant (m s$^{-2}$), *h* is the flow depth (m) and $S_i$ is the sine of the bed slope (m m$^{-1}$).

$$\Omega = \tau V \tag{5}$$

where $\Omega$ is the stream power (W m$^{-2}$), $\tau$ is the shear stress (Pa) and *V* is the mean flow velocity (m s$^{-1}$).

$$P = VS_i \tag{6}$$

where *P* is the unit stream power (m s$^{-1}$), *V* is the mean flow velocity (m s$^{-1}$) and $S_i$ is the sine of the bed slope (m m$^{-1}$).

#### 2.5.5. Mannings roughness

The Manning roughness was calculated by Manning equation (Shih and Rahi, 1982), which was as follows:

$$V = \frac{1}{N}R^{2/3}S_i^{1/2} \tag{7}$$

where *V* is the mean flow velocity (m s$^{-1}$), *N* is the Manning roughness, *R* is the hydraulic radius, and equal to water depth in sheet flow erosion of this study (m) and $S_i$ is the sine of the bed slope (m m$^{-1}$). The manning roughness were from 0.0102 to 0.0620 in this study (Table2).

### 2.6. Data analysis

The data set was divided into two parts, and the size of each data set (n) was 18. One part of the data set was adopted to derive new equations that could describe the relationship of sheet erosion rate with rainfall intensity, slope gradient and the hydraulic parameters via regression analysis, as well as to derive the values of the statistical parameters *R*2 and *NSE*. Another part of the data set was used in equation validation by generating the values of the statistical parameters $R^2$, *RE*, *RME* and *NSE*, which were used to evaluate the performance of new equations. The values of $R^2$, *RE*, *RME* and *NSE* were calculated as follows:

$$RE = \frac{(O_i - P_i)}{O_i} \times 100 \tag{8}$$

$$RME = \frac{1}{n}\sum_{i=1}^{n}\left|\frac{(O_i - P_i)}{O_i}\right| \times 100\% \tag{9}$$

$$R^2 = \frac{\left[\sum_{i=1}^{n}(O_i - \overline{O})(P_i - \overline{P})\right]^2}{\sum_{i=1}^{n}(O_i - \overline{O})^2\sum_{i=1}^{n}(P_i - \overline{P})^2} \tag{10}$$

$$NSE = 1 - \frac{\sum(O_i - P_i)^2}{\sum(O_i - \overline{O})^2} \tag{11}$$

**Table 2**
Mannings roughness for different slope gradients and rainfall intensities.

| Rainfall intensity (mm h$^{-1}$) | Mannings roughness | | | | | |
|---|---|---|---|---|---|---|
| | 12.23% | 17.63% | 26.80% | 36.40% | 40.40% | 46.63% |
| 48 | 0.0204 | 0.0218 | 0.0223 | 0.0235 | 0.0240 | 0.0257 |
| 60 | 0.0102 | 0.0153 | 0.0231 | 0.0264 | 0.0281 | 0.0305 |
| 90 | 0.0114 | 0.0177 | 0.0222 | 0.0300 | 0.0390 | 0.0488 |
| 120 | 0.0153 | 0.0252 | 0.0351 | 0.0375 | 0.0447 | 0.0537 |
| 132 | 0.0165 | 0.0209 | 0.0335 | 0.0401 | 0.0457 | 0.0587 |
| 150 | 0.0168 | 0.0174 | 0.0361 | 0.0438 | 0.0503 | 0.0620 |

where *RE* is the relative error, *RME* is the average absolute values of the relative error, $R^2$ is the coefficient of determination, $O_i$ are the observed values, $P_i$ are the predicted values, $\overline{O}$ is the mean of the observed value, $\overline{P}$ is the mean of the predicted value and *NSE* is the Nash–Sutcliffe model efficiency (Nash and Sutcliffe, 1970). *NSE* is a normalised statistic that reflects the relative magnitude of the residual variance compared with the variance of the observed data [good (*NSE* > 0.7), satisfactory (0.4 < *NSE* ≤ 0.7) and unsatisfactory (*NSE* ≤ 0.4)] (Moriasi et al., 2007; Ahmad et al., 2011; An et al., 2012).

## 3. Results

### 3.1. Sheet erosion rate estimated using slope gradient and rainfall intensity

Fig. 4 shows that sheet erosion rate changes with different slope gradients and rainfall intensities. Evidently, sheet erosion rate was strongly influenced by slope gradient and rainfall intensity. It increased as a power function with slope gradient and rainfall intensity.

For the same slope gradient level, sheet erosion rate clearly increased when rainfall intensity changed from 90 mm $h^{-1}$ to 120 mm $h^{-1}$. Furthermore, for the same rainfall intensity, sheet erosion rate apparently increased when the slope gradient changed from 26.80% to 36.40%.

To evaluate the relationship of sheet erosion rate with slope gradient and rainfall intensity, multivariate regression analyses were conducted to obtain the following relationship using one part of the data set:

$$SE = 7.5 \times 10^{-12} S^{1.43} I^{3.04} (R^2 = 0.91, NSE = 0.80, P < 0.01, n = 18) \quad (12)$$

where *SE* is the sheet erosion (kg $m^{-2}$ $s^{-1}$), *S* is the slope gradient (%) and *I* is the rainfall intensity (mm $h^{-1}$). When the power equations were tested in the regression analysis, log transform was conducted before testing to accurately derive the coefficients and powers of the power equations. Apparently, $R^2$ revealed that *SE* was highly correlated with *S* and *I* (good: $R^2 > 0.8$) and $P < 0.01$ revealed that the relationship of *SE*, *S* and *I* is highly significant (significant: $P < 0.05$); NSE revealed the relative magnitude of the residual variance compared with the variance of the observed data (good: *NSE* > 0.7). Thus, Eq. (12) could be used to predict *SE*, which was satisfied with $R^2 = 0.91$ and *NSE* = 0.80. The validation of Eq. (12) was further achieved using another part of the data set. Fig. 5 shows the validation of Eq. (12) that used another part of the data set and the predicted *SE* is extremely close to the measured values. The validation result further showed that Eq. (12) could be used to predict *SE* accurately with $R^2 = 0.95$ and *NSE* = 0.87 (Table 3). The exponents of slope gradient and rainfall intensity were 1.43 and 3.04, respectively, and the exponent of slope gradient was lower than that of rainfall intensity. Thus, *SE* was more sensitive to rainfall intensity than to slope gradient.

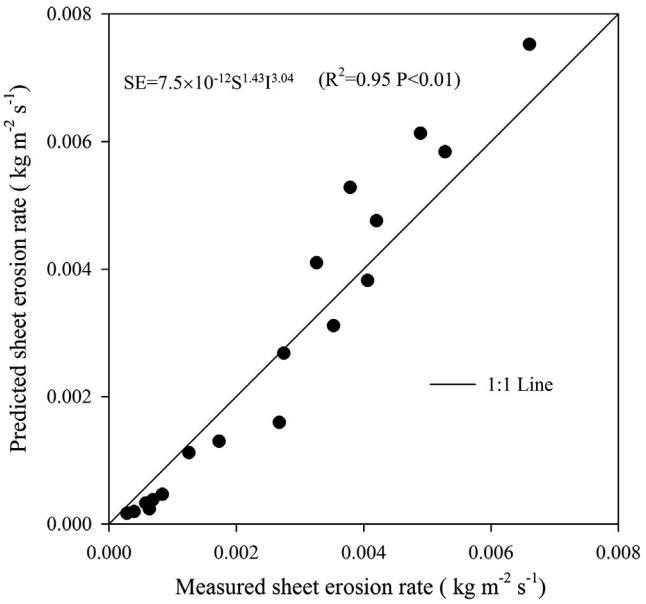


**Fig. 5.** Measured vs. predicted SE (using Eq. (11)).

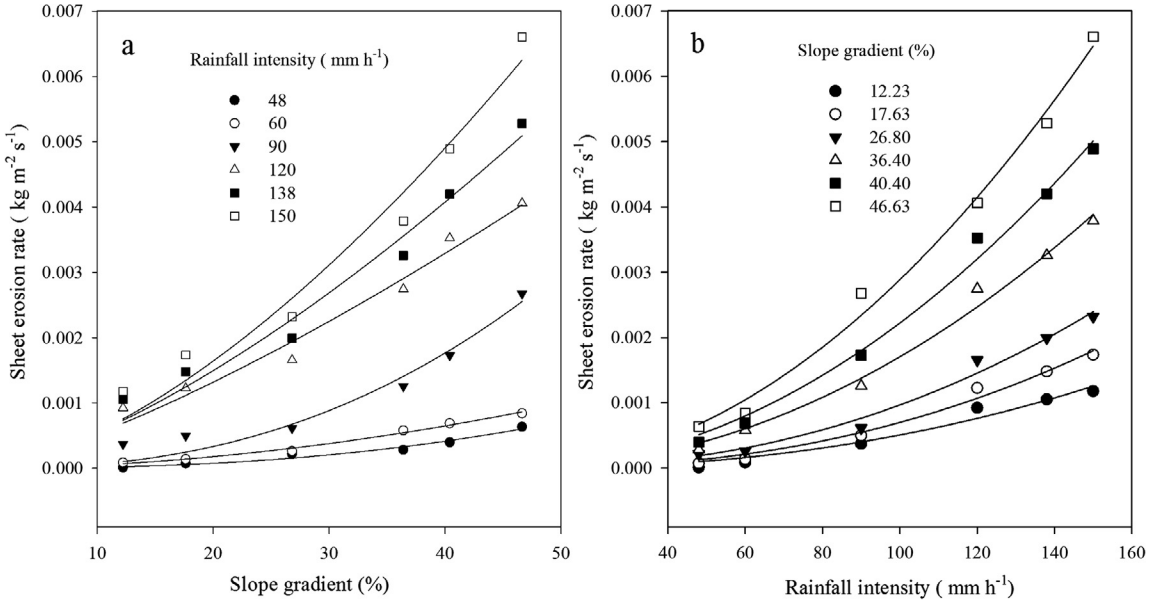


**Fig. 4.** SE as a power function of slope gradient and rainfall intensity.

**Table 3**
The validation of models based on rainfall intensity and slope gradient, flow velocity, hydrodynamic parameters between observed and predicted sheet erosion rate.

| Equation | *RE* (%) | *RME* (%) | $R^2$ | *NSE* | *n* |
|---|---|---|---|---|---|
| $SE = 7.5 \times 10^{-12} S^{1.43} I^{3.04}$ | −39–63 | 28 | 0.95 | 0.87 | 18 |
| $SE = 0.85 V^{3.05}$ | −249–26 | 75 | 0.95 | 0.81 | 18 |
| $SE = 0.011\tau - 0.01$ | −57–116 | 35 | 0.90 | 0.89 | 18 |
| $SE = 0.06\Omega - 0.0003$ | −89–16 | 15 | 0.97 | 0.97 | 18 |
| $SE = 3945 P^{5.04}$ | −237–94 | 77 | 0.73 | -0.05 | 18 |

Where *RE* is the coefficient of relative error, *RME* is the coefficient of mean relative error, $R^2$ is the coefficient of determination and *NSE* is the coefficient of Nash-Suticliffe model efficiency, *n* is the number of the samples.

### 3.2. Sheet erosion rate estimated using flow velocity

Fig. 6 shows that flow velocity changes with different slope gradients and rainfall intensities. Evidently, flow velocity increased as a power function with slope gradient, and the exponents of slope gradient under different rainfall intensities were 0.87, 0.54, 0.50, 0.52, 0.48 and 0.41. Moreover, flow velocity increased as a power function with rainfall intensity, and the exponents of rainfall intensity under different slope gradients were 0.64, 0.60, 0.353, 0.345, 0.347 and 0.297. Thus the flow velocity was more sensitive to slope gradient than to rainfall intensity based on the comparison of the exponents of slope gradient with those of rainfall intensity.

Fig. 7 shows the relationship between sheet erosion rate and flow velocity. Sheet erosion rate is a power function of flow velocity using one part of the data set. The function is expressed as follows:

$$SE = 0.85V^{3.05} (R^2 = 0.82, NSE = 0.82, P < 0.01, n = 18) \quad (13)$$

where *SE* is the sheet erosion rate (kg m$^{-2}$ s$^{-1}$) and *V* is the mean flow velocity (m s$^{-1}$). $R^2$ revealed that *SE* was highly correlated with *V* (good: $R^2 > 0.8$) and $P < 0.01$ revealed that the relationship between *SE* and *V* is highly significant (significant: $P < 0.05$); NSE revealed the relative magnitude of the residual variance compared with the variance of the observed data (good: $NSE > 0.7$). Thus, Eq. (13) could be used to predict sheet erosion rate accurately with $R^2 = 0.82$ and $NSE = 0.82$. Table 3 shows that the validation of Eq. (13) uses another part of the data set. The validation result further exhibited that sheet erosion rate could be predicted using Eq. (13) with $R^2 = 0.95$ and $NSE = 0.81$.

### 3.3. Sheet erosion rate estimated using hydrodynamic parameters

Fig. 8 shows the relationship between sheet erosion rate and shear stress. A linear function existed between shear stress and sheet erosion rate using one part of the data set. The function is provided as follows:

$$SE = 0.011\tau - 0.01 \ (R^2 = 0.88, NSE = 0.88, P < 0.01, n = 18) \quad (14)$$

where *SE* is the sheet erosion rate (kg m$^{-2}$ s$^{-1}$) and $\tau$ is the shear stress (Pa). $R^2$ revealed that *SE* was highly correlated with $\tau$ (good: $R^2 > 0.8$) and $P < 0.01$ revealed that the relationship between *SE* and $\tau$ is highly significant (significant: $P < 0.05$); *NSE* revealed the relative magnitude of the residual variance compared with the variance of the observed data (good: $NSE > 0.7$). Thus, Eq. (14) could be used to predict sheet erosion rate accurately with $R^2 = 0.88$ and $NSE = 0.88$. Table 3 shows the validation of Eq. (14) using another part of the data set. The validation result further demonstrated that Eq. (14) could be used to predict sheet erosion rate accurately with $R^2 = 0.90$ and $NSE = 0.89$.

Fig. 9 shows the relationship between sheet erosion rate and stream power. A linear function existed between stream power and sheet erosion rate using one part of the data set. The function is expressed as follows:

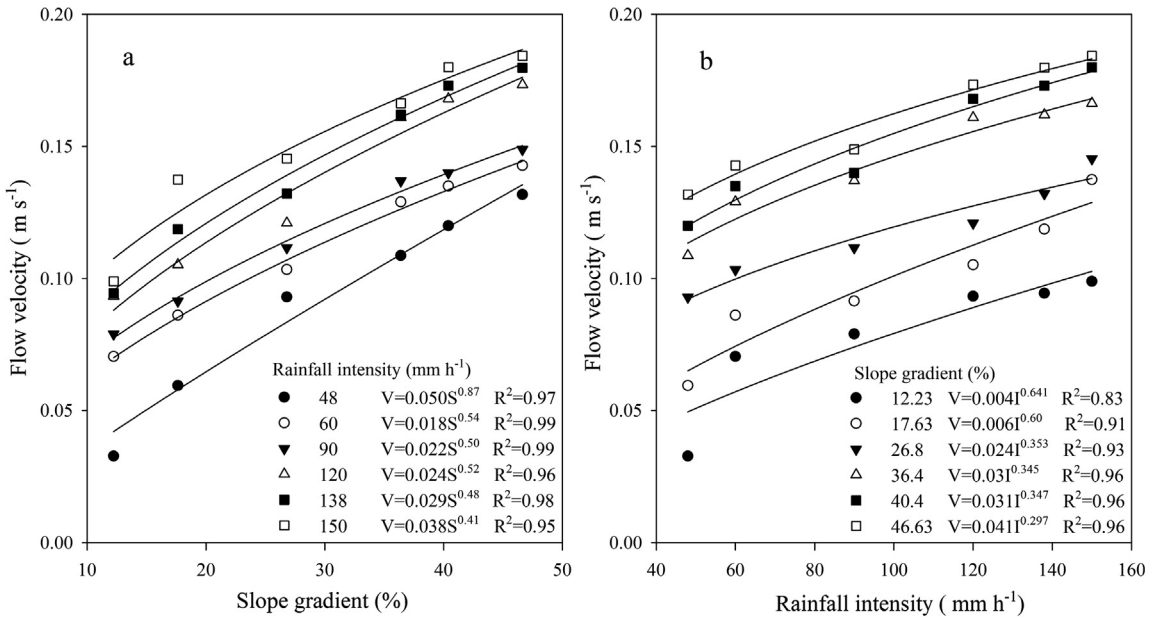


**Fig. 6.** Flow velocity as a power function of slope gradient and rainfall intensity.

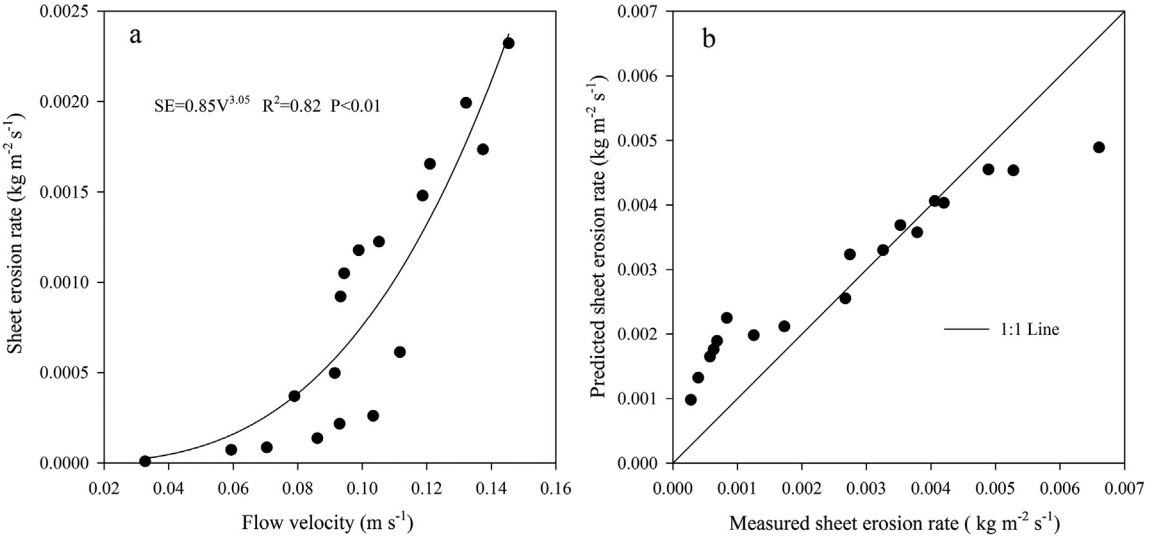


**Fig. 7.** SE as a power function of flow velocity.

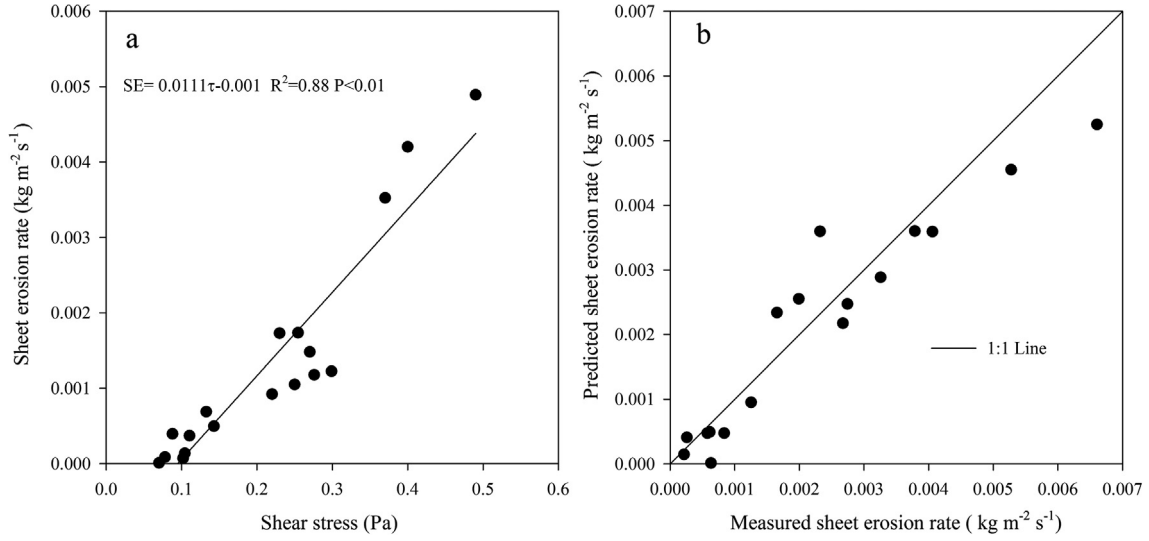


**Fig. 8.** SE as a linear function of shear stress.

$$SE = 0.06\Omega - 0.0003 \ (R^2 = 0.99, NSE = 0.99, P < 0.01, n = 18) \quad (15)$$

where $SE$ is the sheet erosion rate (kg m$^{-2}$ s$^{-1}$) and $\Omega$ is the stream power (W m$^{-2}$). $R^2$ revealed that $SE$ was highly correlated with $\Omega$ (good: $R^2 > 0.8$) and $P < 0.01$ revealed that the relationship between $SE$ and $\Omega$ is highly significant (significant: $P < 0.05$); NSE revealed the relative magnitude of the residual variance compared with the variance of the observed data (good: $NSE > 0.7$). Thus, Eq. (15) could be used to predict the sheet erosion rate accurately with $R^2 = 0.99$ and $NSE = 0.99$. Table 3 shows the validation of Eq. (15) using another part of the data set. The validation result further proved that Eq. (15) could be used to predict sheet erosion rate accurately with $R^2 = 0.97$ and $NSE = 0.97$.

Fig. 10 shows the relationship between sheet erosion rate and unit stream power. A power function existed between unit stream power and sheet erosion rate. The function is provided as follows:

$$SE = 3945P^{5.04} (R^2 = 0.70, NSE = 0.69, P < 0.01, n = 18) \quad (16)$$

where $SE$ is the sheet erosion rate (kg m$^{-2}$ s$^{-1}$) and $P$ is the unit stream power (m s$^{-1}$). $R^2$ revealed that $SE$ was not highly correlated with $P$ (good: $R^2 > 0.8$); NSE revealed the relative magnitude of the residual variance compared with the variance of the observed data and the $NSE$ was not good (good: $NSE > 0.7$). Thus, Unit stream power was not a good predictor of sheet erosion rate with $R^2 = 0.70$ and $NSE = 0.69$. Table 3 shows the validation of Eq. (16) using another part of the data set. The validation result further showed that unit stream power was not a good predictor with $R^2 = 0.73$ and $NSE = -0.05$.

In summary, Table 3 indicates that stream power is the best hydrodynamic parameter for predicting sheet erosion rate.

## 4. Discussion

In this study, rainfall intensity and slope gradient significantly influence sheet erosion rate. In addition, a power function of rainfall intensity and slope gradient can be used to predict sheet

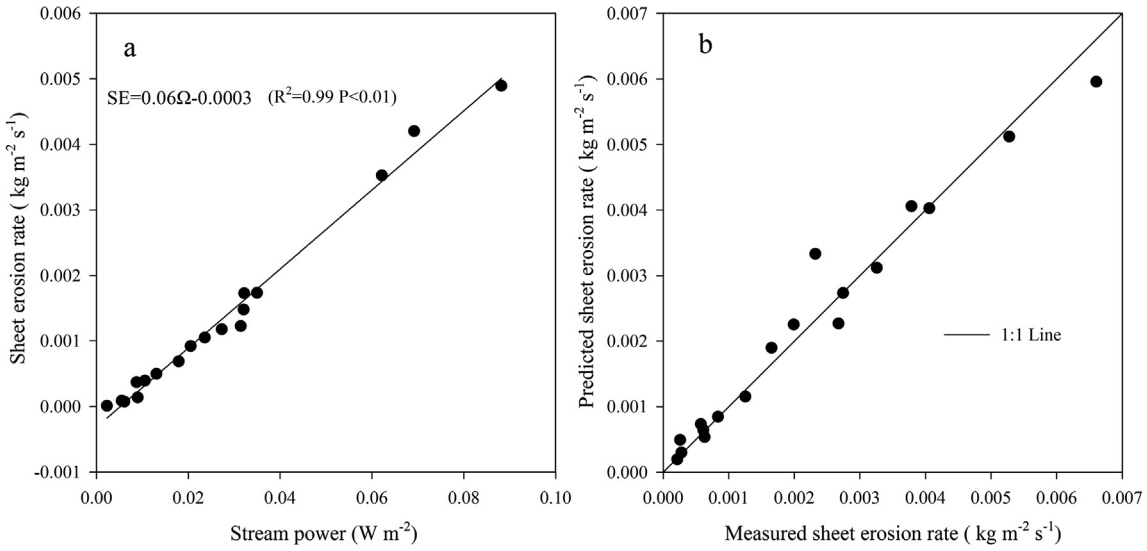


**Fig. 9.** SE as a linear function of stream power.

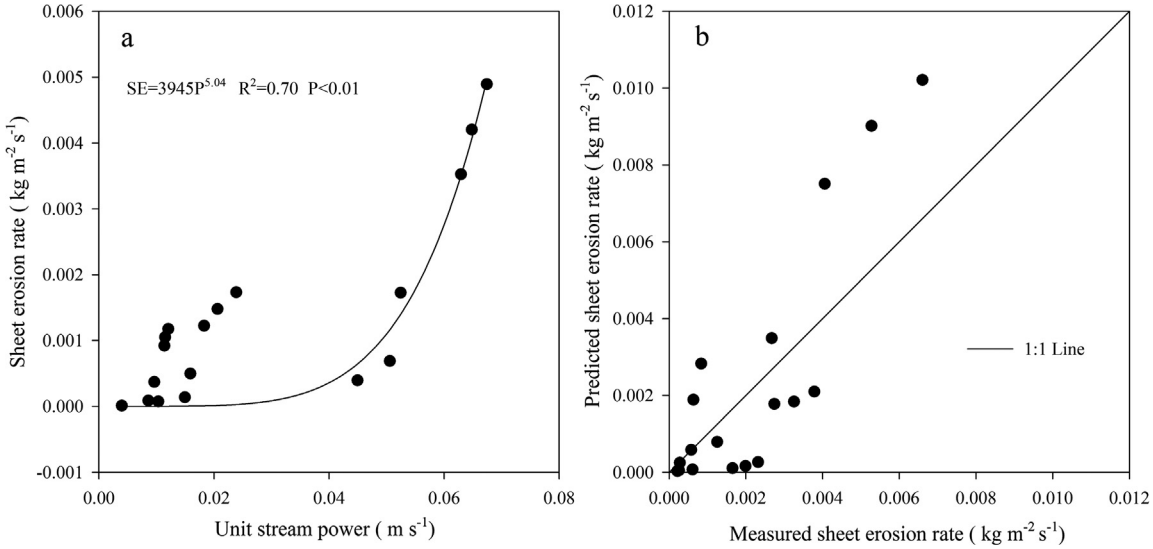


**Fig. 10.** SE as a power function of unit stream power.

erosion rate well. This result is consistent with the reports of other researchers (Mayer, 1981; Kinnell, 1993; Flanagan and Nearing, 1995; Zhang et al., 1998; Fox and Bryan, 2000; Bulygin et al., 2002; Wei et al., 2009). These researchers also used power function equations of rainfall intensity and slope gradient to predict sheet erosion rate (Table 4). However, the exponent of rainfall intensity in these models ranges from 1 to 2, which are less than the exponent (3.04) of rainfall intensity in the current study. The exponent of slope gradient in these models ranges from 0.43 to 1, which are also less than the exponent (1.43) of slope gradient in the current study. Thus, sheet erosion rate is more sensitive to rainfall intensity and slope gradient in our study. Establishing the equation depending on the relationship of sheet erosion rate (*SE*), slope gradient (*S*) and rainfall intensity (*I*) can help to develop erosion prediction models of the Loess Plateau in China.

By contrast, Huang and Bradford (1993) found that the linear functions that existed between sheet erosion rate and slope gradient for three rainfall intensities and slope gradients were 5%, 9% and 20%. The variation in result was likely attributed to slope gradient and soil surface conditions. Firstly, six slope gradients ranging from 12.23% to 46.63% were selected in our study, and thus, the result of the regression analysis could be more accurate. Then, soil surface conditions such as soil moisture, roughness

**Table 4**
Models applied to predict sheet erosion rate.

| Model | Slope exponent | Rainfall intensity exponent |
|---|---|---|
| $SE = K_iI^2$ (Nearing et al., 1989) | – | 2 |
| $SE = K_iIQS$ (Kinnell, 1993) | 1 | 1 |
| $SE = K_iIQS_f$ (Beasley and Huggins, 1982) | – | 1 |
| $SE = K_iIQ^{0.5}S^{0.67}$(Zhang, et al., 1998) | 0.67 | 1 |
| $SE = K_iQ^{2.37}S^{0.43}$ (Fox and Bryan, 2000) | 0.43 | – |
| $SE = K_iIQS^{0.67}$ (Bulygin et al., 2002) | 0.67 | 1 |
| $SE = K_iI^{1.052}Q^{0.592}$ (Wei et al., 2009) | – | 1.052 |
| $SE = 7.5 \times 10^{-12}\ I^{3.04}S^{1.43}$ (This study) | 1.43 | 3.04 |

Where $D_i$ is the sheet erosion rate (kg m$^{-2}$ s$^{-1}$), $K_i$ is soil erodibility (kg m$^{-4}$ s), $I$ is the rainfall intensity (m s$^{-1}$), $Q$ is the runoff rate (m s$^{-1}$), $S$ is slope gradient (m m$^{-1}$), and $S_f$ is a slope adjustment factor.

and slope length significantly affect sheet erosion, which was consistent with the understanding of Assouline and Ben-Hur (2006).

In this study, a power function existed between sheet erosion rate and flow velocity. By contrast, Fox and Bryan (2000) found that a linear function existed between sheet erosion rate and flow velocity. The variation in result was likely attributed to three reasons. Firstly, the flow velocity was highly sensitive to slope gradient, so the steeper slope gradient selected in our study can affect the relationship between sheet erosion rate and flow velocity. Secondly, soil surface roughness is the main factor that affects the flow velocity, which is consistent with the understanding reported by many researchers (Govers, 1992; Nearing et al., 1997; Takken et al., 1998; Nearing et al., 1999; Giménez and Govers, 2001; Ali et al., 2011). Thirdly, soil particles can influence flow velocity, which is consistent with Wu et al. (2016). Thus, steep slope, soil surface roughness and soil particles can influence the relationship between the sheet erosion rate and the flow velocity.

In our study, a linear function existed between sheet erosion rate and shear stress. This result is consistent with the findings of Fox and Bryan (2000). However, the result of the present study is different from that of Fan and Wu (1999), who have observed that a power function existed between sheet erosion rate and shear stress. Because the slope gradient in our study and that reported by Fox and Bryan (2000) were less than 45%, but the slope gradient reported by Fan and Wu (1999) ranged from 10% to 100%, thus the difference on the slope gradient influenced the relationship between sheet erosion rate and shear stress. In our study, a linear function existed between the sheet erosion rate and stream power, which is consistent with the finding reported by Huang (1995) and Cao et al. (2015). The slope gradients reported by Huang (1995) and Cao et al. (2015) ranged from 4% to 26.8%, thus the same relationship between sheet erosion rate and stream power when the slope gradient increased to 46.63%.

## 5. Conclusion

In this study, the relationship of sheet erosion rate with rainfall intensity, slope gradient and hydraulic parameters (i.e. flow velocity, shear stress, unit stream power and stream power) was investigated using simulated rainfall. The results of this study demonstrated that sheet erosion rate increased as a power function with slope gradient and rainfall intensity. Sheet erosion rate was more sensitive to rainfall intensity than to slope gradient. The validation result showed that Eq. (12) could be used to predict sheet erosion rate accurately with $R^2 = 0.95$ and $NSE = 0.87$, as shown in the model calibration and validation.

In addition, flow velocity increased as a power function with slope gradient and rainfall intensity and the exponents of slope gradient ranged from 0.41 to 0.87 and those of rainfall intensity ranged from 0.30 to 0.64. Eq. (13) shows the relationship between sheet erosion rate and flow velocity. The validation result demonstrated that sheet erosion rate could be predicted accurately using Eq. (13) with $R^2 = 0.95$ and $NSE = 0.81$.

The sheet erosion rate could be predicted using linear equations of shear stress and stream power, however, the stream power with $R^2 = 0.99$ and $NSE = 0.99$ was more reliable for predicting sheet erosion rate than shear stress with $R^2 = 0.88$ and $NSE = 0.88$. By contrast, unit stream power was not a good predictor of sheet erosion rate based on the validation result with $R^2 = 0.73$ and $NSE = -0.05$. These findings indicate that stream power is the best hydraulic parameter to predict sheet erosion rate in our study.

Overall, the exiting model can facilitate the prediction of the sheet erosion rate under our study conditions. However, these models should be used judiciously. Thus, the additional research is needed to develop equations/models that can be universally applied to predict sheet erosion rate.

## Acknowledgments

Financial support for this research was provided by the National Natural Science Foundation of China funded project (41471230; 41601282; 41171227); the National Key Research and Development Program of China (2016YFC0402401); Special-Funds of Scientific Research Programs of State Key Laboratory of Soil Erosion and Dryland Farming on the Loess Plateau (A314021403-C2).

## References

Ahmad, H.M.N., Sinclair, A., Jamieson, R., Madani, A., Hebb, B., Havard, P., Yiridoe, E. K., 2011. Modeling sediment and nitrogen export from a rural watershed in Eastern Canada using the soil and water assessment tool. J. Environ. Qual. 40, 1182–1194.

Al-Durrah, M., Bradford, J.M., 1981. New methods of studying soil detachment due to waterdrop impact. Soil Sci. Soc. Am. J. 45 (5), 949–953.

Ali, M., Sterk, G., Seeger, M., Boersema, M.P., Peters, P., 2011. Effect of hydraulic parameters on sediment transport capacity in overland flow over erodible beds. Hydrol. Earth Syst. Sci. Discuss. 8 (4), 6939–6965.

An, J., Zheng, F., Lu, J., Li, G., 2012. Investigating the role of raindrop impact on hydrodynamic mechanism of soil erosion under simulated rainfall conditions. Soil Sci. 177 (8), 517–526.

Assouline, S., Ben-Hur, M., 2006. Effects of rainfall intensity and slope gradient on the dynamics of interrill erosion during soil surface sealing. Catena 66 (3), 211–220.

Bagnold, R.A., 1966. An approach to the sediment transport problem from general physics. US Geol Surv. Prof. Pap. 422 (1), 22–37.

Beasley, D.B., Huggins, L.F., 1982. ANSWERS user's manual. Dep. of Agric. Eng., Purdue Univ., West Lafayette, IN.

Bulygin, S.Y., Nearing, M.A., Achasov, A.B., 2002. Parameters of interrill erodibility in the WEPP model. Eurasian Soil Science C/C of Pochvovedenie 35 (11), 1237–1242.

Cantalice, J.R.B., Silveira, F.P.M., Singh, V.P., Silva, Y.J.A.B., Cavalcante, D.M., Gomes, C., 2016. Interrill erosion and roughness parameters of vegetation in rangelands. Catena.

Cao, L., Zhang, K., Dai, H., Liang, Y., 2015. Modeling interrill erosion on unpaved roads in the loess plateau of China. Land Degrad. Dev. 26 (8), 825–832.

Fan, J.C., Wu, M.F., 1999. Effects of soil strength, texture, slope steepness and rainfall intensity on interrill erosion of some soils in Taiwan. In: 10th International Soil Conservation Organization meeting, Purdue University, USDA-ARS National Soil Erosion Research Laboratory.

Fox, D.M., Bryan, R.B., 2000. The relationship of soil loss by interrill erosion to slope gradient. Catena 38 (3), 211–222.

Flanagan, D.C., Nearing, M.A., 1995. USDA-Water Erosion Prediction Project: Hillslope profile and watershed model documentation (vol. 10). NSERL report.

Giménez, R., Govers, G., 2001. Interaction between bed roughness and flow hydraulics in eroding rills. Water Resour. Res. 37 (3), 791–799.

Govers, G., 1992. Evaluation of transporting capacity formulae for overland flow. University College London Press, London, pp. 243–273.

Huang, C., Bradford, J.M., 1993. Analyses of slope and runoff factors based on the WEPP erosion model. Soil Sci. Soc. Am. J. 57 (5), 1176–1183.

Huang, C.H., 1995. Empirical analysis of slope and runoff for sediment delivery from interrill areas. Soil Sci. Soc. Am. J. 59 (4), 982–990.

Huang, G.H., Zhan, W.H., 2002. Fractal property of soil particle size distribution and its application. Acta Pedol. Sin. 39 (4), 490–497 (in Chinese).

Kinnell, P.I.A., 1990. Modelling erosion by rain-impacted flow. In: Bryan, R.B. (Ed.), Soil Erosion, Experiments and Models, pp. 55–66. Catena Supplement 17.

Kinnell, P.I.A., 1993. Interrill erodibilities based on the rainfall intensity flow discharge erosivity factor. Aust. J. Soil Res. 31 (3), 319–332.

Li, G., Abrahams, A.D., 1999. Controls of sediment transport capacity in laminar interrill flow on stone-covered surfaces. Water Resour. Res. 35 (1), 305–310.

Liu, B.Y., Nearing, M.A., Risse, L.M., 1994. Slope gradient effects on soil loss for steep slopes. Trans. ASAE 37 (6), 1835–1840.

Liu, J.E., Wang, Z., Gao, S., Zhang, K., 2012a. Experimental study on hydro-dynamic mechanism of sheet erosion processes on loess hillslope. Trans. Chin. Soc. Agric. Eng. 28 (7), 144–149 (in Chinese).

Liu, J.E., Wang, Z.L., Yang, X.M., Jiao, N., Shen, N., Ji, P.F., 2014. The impact of natural polymer derivatives on sheet erosion on experimental loess hillslope. Soil Tillage Res. 139, 23–27.

Liu, Y., Fu, B., Lü, Y., Wang, Z., Gao, G., 2012b. Hydrological responses and soil erosion potential of abandoned cropland in the Loess Plateau China. Geomorphology 138 (1), 404–414.

McCool, D., Brown, L., Foster, G., Mutchler, C., Meyer, L., 1987. Revised slope steepness factor for the Universal Soil Loss Equation. Trans. Am. Soc. Agric. Eng. 30, 1387–1396.

Meyer, L.D., 1981. How rain intensity affects interrill erosion. Trans. ASAE 24, 1472–1475.
Misra, R.K., Rose, C.W., 1996. Application and sensitivity analysis of process-based erosion model GUEST. Eur. J. Soil Sci. 47 (4), 593–604.
Morgan, R.P.C., Quinton, J.N., Smith, R.E., Govers, G., Poesen, J.W.A., Auerswald, K., Styczen, M.E., 1998. The European soil erosion model (EUROSEM): a dynamic approach for predicting sediment transport from fields and small catchments. Earth Surf. Proc. Land. 23 (6), 527–544.
Moriasi, D.N., Arnold, J.G., Van Liew, M.W., Bingner, R.L., Harmel, R.D., Veith, T.L., 2007. Model evaluation guidelines for systematic quantification of accuracy in watershed simulations. Trans. ASABE 50 (3), 885–900.
Moss, A.J., 1988. The effects of flow–velocity variations on rain-driven transportation and the role of rain impact in the movement of solids. Aust. J. Soil Res. 26, 443–450.
Nash, J., Sutcliffe, J.V., 1970. River flow forecasting through conceptual models part I—A discussion of principles. J. Hydrol. 10 (3), 282–290.
Nearing, M.A., Bradford, J.M., Parker, S.C., 1991. Soil detachment by shallow flow at low slopes. Soil Sci. Soc. Am. J. 55, 339–344.
Nearing, M.A., Foster, G.R., Lane, L.J., Finkner, S.C., 1989. A process-based soil erosion model for USDA-Water Erosion Prediction Project technology. Trans. ASAE 32, 1587–1593.
Nearing, M.A., Norton, L.D., Bulgakov, D.A., Larionov, G.A., West, L.T., Dontsova, K.M., 1997. Hydraulics and erosion in eroding rills. Water Resour. Res. 33 (4), 865–876.
Nearing, M.A., Simanton, J.R., Norton, L.D., Bulygin, S.J., Stone, J., 1999. Soil erosion by surface water flow on a stony, semiarid hillslope. Earth Surf. Proc. Land. 24, 677–686.
Prosser, I.P., Rustomji, P., 2000. Sediment transport capacity relations for overland flow. Prog. Phys. Geogr. 24, 179–193.
Shen, H., Zheng, F., Wen, L., Han, Y., Hu, W., 2016. Impacts of rainfall intensity and slope gradient on rill erosion processes at loessial hillslope. Soil Till. Res. 155, 429–436.
Shi, H., Shao, M., 2000. Soil and water loss from the loess plateau in China. J. Arid Environ. 45 (1), 9–20.
Shih, S.F., Rahi, G.S., 1982. Seasonal variations of Manning's roughness coefficient in a subtropical marsh. Trans. ASAE 25 (1), 116–119.
Takken, I., Govers, G., Ciesiolka, C.A.A., Silburn, D.M., Loch, R.J., 1998. Factors influencing the velocity-discharge relationship in rills. IAHS Publ., 63–70
Wei, H., Nearing, M.A., Stone, J.J., Guertin, D.P., Spaeth, K.E., Pierson, F.B., Nichols, M. H., Moffet, C.A., 2009. A new splash and sheet erosion equation for rangelands. Soil Sci. Soc. Am. J. 73 (4), 1386–1392.
Wu, B., Wang, Z., Shen, N., Wang, S., 2016. Modelling sediment transport capacity of rill flow for loess sediments on steep slopes. Catena 147, 453–462.
Yang, C.T., 1972. Unit stream power and sediment transport. J. Hydr. Div. 98 (10), 1805–1826.
Yang, C.T., 1973. Incipient motion and sediment transport. J. Hydr. Div. 99 (10), 1679–1704.
Zhang, G.H., Liu, Y.M., Han, Y.F., Zhang, X.H., 2009. Sediment transport and soil detachment on steep slopes: I. Transport capacity estimation. Soil Sci. Soc. Am. J. 73 (4), 1291–1297.
Zhang, K.L., Hosoyamada, K., 1996. Influence of slope gradient on interrill erosion of Shirasu soil. Soil Phys. Conditions Plant Growth Jpn. 73, 37–44.
Zhang, X.C., Nearing, M.A., Miller, W.P., Norton, L.D., West, L.T., 1998. Modeling interrill sediment delivery. Soil Sci. Soc. Am. J. 62, 438–444.
Zhao, G., Mu, X., Wen, Z., Wen, Z., Wang, F., Gao, P., 2013. Soil erosion, conservation, and eco-environment changes in the loess plateau of China. Land Degrad. Dev. 24 (5), 499–510.